Test of Particle-Assisted Tunneling for Strongly Interacting Fermions in an Optical Superlattice

T. Goodman, L.-M. Duan
FOCUS center and MCTP, Department of Physics, University of Michigan, Ann Arbor, MI 48109

Fermions in an optical lattice near a wide Feshbach resonance are expected to be described by an effective Hamiltonian of the general Hubbard model with particle-assisted tunneling rates resulting from the strong atomic interaction [Phys. Rev. Lett. 95, 243202 (2005)]. Here, we propose a scheme to unambiguously test the predictions of this effective Hamiltonian through manipulation of ultracold atoms in an inhomogeneous optical superlattice. The structure of the low-energy Hilbert space as well as the particle assisted tunneling rates can be inferred from measurements of the time-of-flight images.

Fermions in an optical lattice near a wide Feshbach resonance provide one of the most complicated systems for ultracold atoms [1, 2, 3, 4, 5, 6, 7, 8, 9]. The strong atomic interaction induced by Feshbach resonance populates many excited lattice bands and causes direct couplings between neighboring sites. To understand this important system, one needs to have a theoretical model. An effective Hamiltonian has been proposed in Refs. [5, 9] based on the arguments of the low-energy Hilbert space structure, which offers a significant simplification for description of this system. The effective Hamiltonian takes the form of the general Hubbard model (GHM), where the effects of the multiband populations and the direct neighboring interactions are incorporated through the particle-assisted tunneling rates. It is important to test this model by comparing its predictions with experimental observations. However, such a comparison is usually difficult because of the lack of exact solutions to the GHM and complications in real experimental configurations (such as the inhomogeneity due to the global trap).

In this paper, we propose an experimental scheme to quantitatively test the predictions of this effective model by manipulating strongly interacting atoms in an optical superlattice. The optical superlattice provides a powerful tool, which has been used in recent experiments for demonstration of the spin super-exchange interaction [10, 11, 12]. In the experimental configuration with an inhomogeneous optical superlattice, through manipulation of the lattice barrier and the external magnetic field, we show that one can reconstruct the two-site dynamics from the measured time-of-flight images. The measured dynamics can then be compared with the exact prediction from the general Hubbard model, offering an unambiguous testbed for this complicated system. The proposed measurement also allows a complete empirical determination of all the parameters in the effective GHM.

We consider two component fermions (denoted by spin $\sigma =\uparrow,\downarrow$) in an optical lattice near a wide Feshbach resonance. Although in general many lattice bands get populated due to the strong atomic interaction, we note in Refs. [5, 9] that for this system the low energy states at each site are still restricted to only four possibilities: either a vacuum denoted by $|0\rangle$, or a single atom with spin-σ denoted by $a_\sigma^\dagger|0\rangle$, or a dressed molecule in the ground state $|d\rangle$ which consists of superpositions of two-atom states distributed over many bands. All the other states (such as the three-atom states or the dressed molecule excited states) are well separated in energy, and therefore not relevant for low-temperature physics. Based on this low-energy Hilbert space structure and general symmetry arguments, it is shown in [9] that the effective Hamiltonian takes the form of the GHM:

$$H=\sum_i\left[(U/2)\,n_i\,(n_i-1)-\mu_i n_i\right] \qquad (1)$$
$$+\sum_{\langle i,j\rangle,\sigma}\left[t_a+g_1\,(n_{i\overline{\sigma}}+n_{j\overline{\sigma}})+g_2 n_{i\overline{\sigma}}n_{j\overline{\sigma}}\right]a_{i\sigma}^\dagger a_{j\sigma}+H.c.$$

where $n_i\equiv\sum_\sigma a_{i\sigma}^\dagger a_{i\sigma}$, $n_{i\overline{\sigma}}\equiv a_{i\overline{\sigma}}^\dagger a_{i\overline{\sigma}}$ ($\overline{\sigma}=\downarrow,\uparrow$ for $\sigma=\uparrow,\downarrow$), U characterizes the effective on-site interaction (defined as the energy shift of $|d\rangle$ with respect to the two-atom state on different sites), μ_i is the chemical potential (we keep its dependence on the site i for convenience of the following discussion, where a global trap induces a site dependent energy shift), t_a is the conventional single-atom tunneling rate, and g_1 and g_2 denote the additional tunneling assisted with spin-$\overline{\sigma}$ atoms (those two terms come from the multi-band populations in the $|d\rangle$ state and the direct neighboring atomic interaction in the lattice [5]). In this derivation, we have mathematically mapped $|d\rangle$ to the double occupation state $a_{i\uparrow}^\dagger a_{i\downarrow}^\dagger|0\rangle$ [9] (though their physical compositions are different).

To see whether the effective GHM gives a good description of the low-temperature physics for this system, it is important to test the predictions of the GHM through experiments. To have an unambiguous test, it is better to design a configuration such that the GHM allows exact solutions. The optical superlattice provides such an opportunity. To produce the optical superlattice, one simply adds a 3-dimensional lattice $V_2=V_{20}\sum_{\alpha=x,y,z}\sin^2(\pi\alpha/2a)$ to a lattice $V_1=V_{10}\sin^2(\pi z/a-\varphi)$ in one spatial direction (say z), where the periodicity $2a$ of V_2 is twice that of V_1[10, 11, 12]. If V_{10} is sufficiently large relative to V_{20}, the superposition of these two potentials produces a series of double wells along the z direction. The dynamics in each double well are independent of the others provided the barrier between wells (controlled by V_{20}) is sufficiently large.

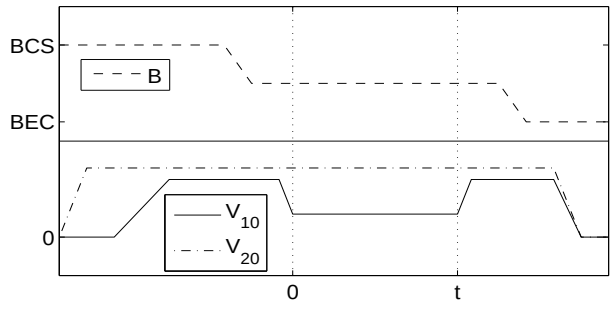

FIG. 1: The time sequences for the magnetic field (B) and the lattice potentials (V_{10} and V_{20}) to achieve state preparation, controlled dynamics, and detection. (Note that the optical barriers are high during sweeping of the B field.)

Taking the relative phase φ to be nonzero introduces an energy bias δ_{12} between the minima of each double well.

It is easy to calculate the dynamics in each double well from the GHM. However, it is unclear how to directly measure the dynamics without individual addressing of each well inside the lattice. The conventional time-of-flight (ToF) images involve averages over all the potential wells. These signals are further complicated by the presence of a global harmonic trap $V_g = \sum_{\alpha=x,y,z} m\omega_\alpha^2\alpha^2/2$ inevitable in an optical lattice, which makes each double well slightly different. In the following, we show a scheme that can map out the detailed dynamics in each double well from the measured ToF images even with the presence of these complications.

The scheme here combines the control of both the optical potentials and the magnetic field (see Fig. 1 for illustration). First, we need to load each double well with a filling pattern that sets the initial condition of the dynamics. This is achieved at the BCS limit of the resonance. In this limit, the atoms are free fermions, and we can control the filling pattern by choosing the total number $N = N_\uparrow + N_\downarrow$ and the polarization $P = (N_\uparrow - N_\downarrow)/N$. Then, we turn off all the inter-well dynamics by raising the barrier (controlled by V_{10} and V_{20}) and sweep the magnetic field to the unitarity region. The sweeping speed v is fast compared with the inter-well coupling rate but small compared with the lattice gap of V_1 so that the levels in each single well adiabatically evolve. Near unitarity, we turn on the inter-well dynamics for a duration t by adjusting V_{10} to lower the central barrier of each double well. These dynamics give information on the underlying strongly interacting Hamiltonian. To determine the final state after the dynamics, the central barrier is raised again, and the magnetic field is swept to the BEC limit with a speed similar to v. Depending on the particle number in each well, we have atoms or molecules or their mixture with negligible interaction at the BEC limit. The ToF images for those atoms or molecules are then detected to determine the final state after the dynamics during time t.

To test the prediction of particle-assisted tunneling, we need to compare the free-atom hopping rate t_a with $t_{a2} = t_a + g_1$ and $t_{a3} = t_a + 2g_1 + g_2$, where t_{a2} and t_{a3} correspond respectively to the hopping rates of a spin-$\uparrow$ atom from the site i to j when there is a spin-$\downarrow$ atom on one site or on both sites. Let us first look at how to measure the free-atom hopping rate t_a in the Hamiltonian (1). For that purpose, we need one atom per double well. By choosing the polarization $P = 1$ and $V_{10} = 0$ (so we have at this stage single wells rather than double wells), the equilibrium distribution of the free fermions at the BCS limit automatically gives this configuration. The total atom number N within the global harmonic trap V_g needs to be below

$$N_{max} = (4\pi/3)\left(E_{bg}/2m\omega^2a^2\right)^{3/2}, \qquad (2)$$

where $E_{bg} = 2\sqrt{V_{10}\pi^2\hbar^2/8ma^2}$ is the band gap for the lattice V_2 and we have assumed $\omega_x = \omega_y = \omega_z \equiv \omega$. Then, one can adiabatically raise the potential V_{10} with a bias δ_{12} so that the atom sits on the left-side well in each double well. After raising V_{10}, δ_{12} is reduced to zero. The system is then moved to the resonance region, and after turn-on of the dynamics for a duration t, the difference between the fraction of atoms in the left-side and the right-side wells over the whole harmonic trap is given by

$$\frac{N_L - N_R}{N} = 1 - \frac{2}{N}\sum_i \left(\frac{t_a}{\hbar\Omega_{1i}}\right)^2 \sin^2(\Omega_{1i}t), \qquad (3)$$

where $\Omega_{1i} = \sqrt{\Delta_i^2 + 4t_a^2}/2\hbar$, $\Delta_i \approx m\omega^2 a z_i$. The summation of i in Eq. (3) is over all the occupied double wells in the global harmonic trap (with z_i the z-coordinate of the center of the double well), and each double well has a slightly different bias Δ_i due to the trap potential V_g. After the dynamics, in order to measure the populations N_L and N_R, the atom of the right-side well can be dumped into an excited vibrational state (corresponding to the second band) of the left-side well by rapidly raising the potential minimum of the right well relative to the left (through control of the phase φ) [10, 11, 12]. The populations in different bands are then mapped out in the BEC limit through measurement of the momentum distribution of free atoms with ToF imaging. From the measured populations N_L and N_R, one can easily determine the tunneling rate t_a. Fig. 2 (a) shows the typical time evolution of $N_L - N_R$ from the dynamics, for which the oscillation period is determined by t_a and the damping is due to the inhomogeneity from the global trap [13]. In the frequency domain, the signal peaks at $2t_a$, and the inhomogeneity causes many smaller peaks at frequencies above that of the dominant peak (see Fig. 2 (b)).

To measure the particle-assisted tunneling rate t_{a2}, we need two atoms per double well, one spin-$\uparrow$ and one spin-$\downarrow$. This can be achieved with the equilibrium distribution of free fermions at the BCS limit by choosing $P \approx 0$, $V_{10} = 0$, and the total atom number $N < 2N_{max}$ (with N_{max} defined in Eq. 2). The double well is still turned on with a bias so that both of the atoms are prepared in

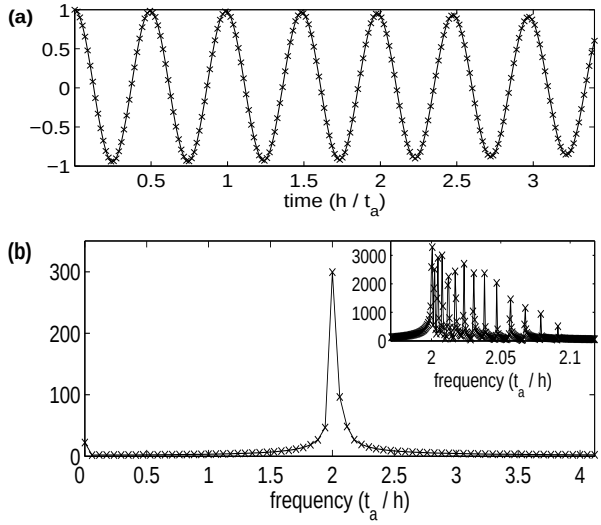

FIG. 2: Population difference between the left and right wells $(N_L - N_R)/N$ for the case of one atom per double well. **(a):** Population difference vs. time (in the unit of h/t_a). **(b):** Fourier transform of the population difference (frequency in the unit of t_a/h), calculated for a time duration of $20h/t_a$ to give a frequency resolution of $t_a/20h$. The peak occurs at a frequency $\nu = 2t_a/h$. **Inset:** With the time duration increased to give a frequency resolution of $t_a/2000h$, we see that there are actually many peaks, corresponding to the different frequencies Ω_{1i}. Ω_{1i} depends on the z-coordinate and thus each peak corresponds to a different slice of double wells parallel to the z-axis. The slices containing the most occupied double wells are closest to $z = 0$. That is why those peaks (which have the smallest Ω_{1i}) dominate. Because t_a can be determined from the dominant peak, it is not necessary to resolve the other smaller peaks. In calculation of the inhomogeneity effect, we assume a spherical distribution with a diameter of 30 occupied double wells, and take the following typical values for the parameters: $t_a = h \times 170$ Hz, $m = 6.64 \times 10^{-26}$ kg (for ^{40}K), $\omega = 2\pi \times 80$ Hz, and $2a = 765$ nm.

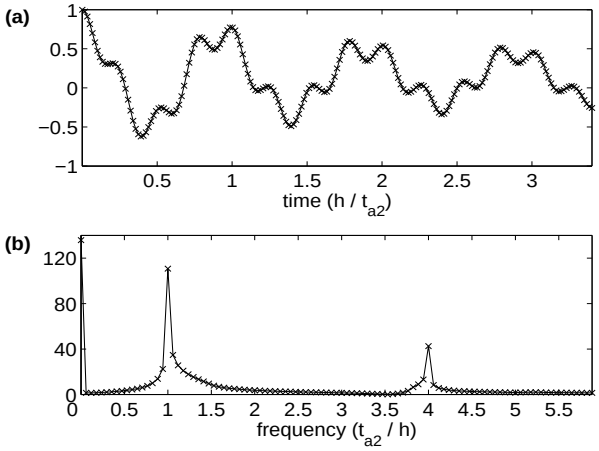

FIG. 3: The difference between the fractions of doubly occupied left and right wells $(N_{2L} - N_{2R})/(N_{2L} + N_{2R})$ for the case of two atoms per double well. **(a):** Population difference vs. time (in the unit of h/t_{a2}). **(b):** Fourier transform of the population difference (the frequency resolution is 1/20 in the unit of t_{a2}/h. The peaks occur at a frequencies $\nu_1 = \left(\sqrt{U^2 + 16t_{a2}^2} - U\right)/2h$ and $\nu_2 = \left(\sqrt{U^2 + 16t_{a2}^2} + U\right)/2h$ (in the figure we take $U = 3t_{a2}$ as an example). Increasing the frequency resolution would reveal a series of smaller peaks on the high frequency side of the large peaks (as in Fig. 2), but it is not necessary to resolve these smaller peaks to determine t_{a2} and U.

the left-side well. For the dynamics near resonance with the Hamiltonian (1), the state at any time involves a superposition of three components: a double occupation of the left or the right well, and a singlet state of two atoms over the two wells. We can determine t_{a2} as well as the on-site interaction energy U from the difference between the overall fractions of double occupation of the left wells and of the right wells, $(N_{2L} - N_{2R})/(N_{2L} + N_{2R})$. (Here N_{2L} and N_{2R} are the total number of double wells in which the left and right wells, respectively, are doubly occupied.) These fractions can be directly measured at the BEC limit, where the double occupation of a site is mapped to a molecule state, and the molecules in the left and the right wells are distinguished through the band mapping and the measurement of the momentum distribution (similar to the discussion above for the atomic case). The single-atom occupation of a well is mapped to an atomic state at the BEC limit. Because of the large detuning between the atomic and the molecular state, the atomic population does not contribute to the time-of-flight imaging signal of the molecular fraction.

The typical time evolution of $(N_{2L} - N_{2R})/(N_{2L} + N_{2R})$ is shown in Fig. 3 (a). In the frequency domain (see Fig. 3 (b)), one can see two distinct primary peaks in the Fourier transform, centered at $\left(\sqrt{U^2 + 16t_{a2}^2} \pm U\right)/2$. The smaller peaks from the inhomogeneity of the global harmonic trap do not obscure these two dominant peaks. The frequencies at which these two peaks occur can be understood by the fact that while the oscillation frequency varies from well to well due to the z-dependent bias, there are a greater number of occupied double wells near $z = 0$ than for any other z-coordinate. Thus, the dominant peaks correspond to the zero bias case, where we have

$$\frac{N_{2L}^{(0)} - N_{2R}^{(0)}}{N_{2L}^{(0)} + N_{2R}^{(0)}} = \frac{\Omega_+}{\Omega} \cos(\Omega_- t) + \frac{\Omega_-}{\Omega} \cos(\Omega_+ t), \qquad (4)$$

with $\Omega_\pm = (\hbar\Omega_{2i} \pm U)/2\hbar$ and $\Omega_{2i} = \sqrt{U^2 + 16t_{a2}^2}/\hbar$.

One can also measure the parameter g_2 in the Hamiltonian (1), which requires three atoms per double wells (two spin-↑, one spin-↓). One can consider this case as a single spin-↑ hole in each double wells, with a hole hopping rate of t_{a3}. This hopping rate can be measured by the same method as for measurement of the free atom hopping rate t_{a1}. To prepare three atoms per double wells, one can consider the free fermion distribution at the BCS limit in an asymmetric double-well lattice with

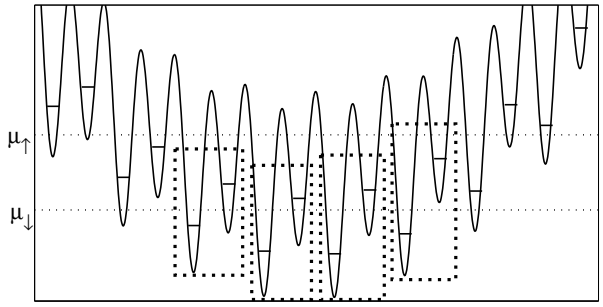

FIG. 4: The superlattice configuration to achieve three atoms per double well. This is obtained by turning on the lattice potentials V_1 and V_2 simultaneously with relative phase $\varphi > 0$, producing double wells with a non-zero potential bias between the left and right wells. (The overall harmonic potential is exaggerated for illustration purposes). In the figure, the solid line in each well corresponds to the lowest level, the long dotted lines correspond to the Fermi surfaces for ↑-atoms and ↓-atoms (with Fermi energies $\mu_\uparrow$ and $\mu_\downarrow$), which differ due to the polarization $P > 0$, and the dotted rectangles indicate those double wells that are occupied by two ↑-atoms and one ↓-atom. The $\mu_\uparrow$ and $\mu_\downarrow$ are chosen such that ↓-atoms only occupy the left wells while ↑-atoms occupy both wells. This is the initial configuration needed to measure the hole hopping rate t_{a3}. There is also the possibility of additional ↑-atoms further from the center of the trap, but the measured molecule signal is only sensitive to double wells containing *both* ↑-atoms and ↓-atoms. With the conditions given in the text, we insure that the only such double wells are those with two ↑-atoms and one ↓-atom.

a bias δ_{12} controlled by the phase shift φ. We would like to have two atoms (one spin-↑ and one spin-↓) in the deep wells and one spin-↑ atom in the shallow wells as shown in Fig. 4. This can be achieved by choosing the polarization P and bias δ_{12} so that the atom numbers satisfy $N_\uparrow > \left(2\sqrt{2}+1\right) N_0$ and $N_\downarrow < N_0$, where $N_0 = (4\pi/3)\left(\delta_{12}/2m\omega^2 a^2\right)^{3/2}$. These relations were derived by requiring that $N_\uparrow$ be great enough that every double well which contains a ↓-atom must also contain at least two ↑-atoms (so that the molecule signal corresponds only to double wells containing three atoms), and also requiring that no double well contain more than one ↓-atom. (Note that it is not sufficient to require a polarization $P \geq 1/3$, since this could be achieved with an inner core of double wells containing one ↑-atom and one ↓-atom, surrounded by a shell of double wells containing only an ↑-atom.) $N_\uparrow$ must also be small enough that there are no more than two ↑ atoms per double well in the center of the trap. This condition can be met along with the above conditions provided the band gap of the lattice is sufficiently great.

A key assumption in deriving the Hamiltonian (1) is that in the strongly interacting region there is a significant energy gap (of the order of the band gap) which separates the four low energy states on each site from the other higher energy states [5, 9]. With the superlattice technique, one can directly test this assumption and measure the energy gap. Given this energy gap, if we fill each site with two atoms, there will be no dynamics as long as the atomic tunneling rate between the two sites is small compared with the band gap energy. To fill each site with two atoms (one spin-↑, one spin-↓), we can start with the free-fermion distribution in the BCS limit, choosing the polarization $P \approx 0$ and total atom number $N < 4N_{max}$ (with N_{max} as defined in Eq. 2). We then adiabatically turn on V_1 and V_2 simultaneously while keeping a constant ratio $V_{10}/V_{20} > 1$. With this filling pattern, we should see no dynamics in the strongly interacting region, so the atomic distribution over the two sites (which will be mapped to the molecular population distribution in the BEC limit) will not change with the evolution time t. One can also tilt the double-well lattice by tuning the bias δ_{12}, and measure what is the critical δ_{12} to turn on the two-site dynamics in the population distribution. The measured critical δ_{12} will give an estimate of the energy gap to excite the system to the high energy states.

In summary, we have described a scheme to test in a controllable fashion the predictions of an effective Hamiltonian for strongly interacting fermions in an optical lattice. With the superlattice technique, one can directly test the key assumption in derivation of the Hamiltonian, and can measure the physical parameters to confirm the particle-assisted tunneling. This scheme provides a quantitative testbed to compare theory with experiments in the strongly interacting region.

This work is supported under the MURI program and under ARO Award W911NF0710576 with funds from the DARPA OLE Program.

[1] J. K. Chin et al., Nature **443**, 961 (2006).
[2] T. Stoeferle et al., Phys. Rev. Lett. **96**, 030401 (2006).
[3] D. B. M. Dickerscheid et al., Phys. Rev. A **71**, 043604 (2005).
[4] L. Carr and M. Holland, Phys. Rev. A **72**, 031604 (2005).
[5] L.-M. Duan, Phys. Rev. Lett. **95**, 243202 (2005).
[6] R. B. Diener and T.-L. Ho, Phys. Rev. Lett. **96**, 010402 (2006).
[7] F. Zhou and C. Wu, New J. Phys. **8**, 166 (2006).
[8] E. G. Moon, P. Nikolic, S. Sachdev, Phys. Rev. Lett. **99**, 230403 (2007).
[9] L.-M. Duan, Euro. Phys. Lett. **81**, 20001 (2008).
[10] S. Folling et al., Nature **448**, 1029 (2007).
[11] M. Anderlini, et al., Nature 448, 452 (2007).
[12] S. Trotzky et al., Science, **319**, 295 (2008).
[13] Note that in this case, the dynamics should be the same as the bosonic case, and the latter has been measured in recent experiments [10].